Chinese Journal of Polymer Science Vol. 30, No. 2, (2012), 269–277

Chinese Journal of Polymer Science

EFFECT OF POLY(BUTYLENE SUCCINATE) ON THE MORPHOLOGY EVOLUTION OF POLY(VINYLIDENE FLUORIDE) IN THEIR BLENDS*

Tian-chang Wang
State Key Laboratory of Polymer Physics and Chemistry, Institute of Chemistry, The Chinese Academy of Sciences, Beijing 100190, China
Hui-hui Li** and Shou-ke Yan
State Key Laboratory of Chemical Resource Engineering, Beijing University of Chemical Technology, Beijing 100029, China

Abstract The effect of PBS on the morphological features of PVDF has been investigated by optical and atomic force microscopies under various conditions. It was found that neat PVDF forms large γ form spherulites with extraordinarily weak birefringence at 170°C. Adding 30% PBS makes PVDF exhibit intrigued flower-like spherulitic morphology. The growth mechanism was explained by the decrease of the supercooling and the materials dissipation. Increasing the PBS content to 70% favors the formation of ring banded spherulites. Temperature dependent experiments verify the $\alpha \rightarrow \gamma'$ phase transition occurs from the junction sites of the α and γ crystals, while starts from the centers of α spherulites in the blends. Ring banded structures could be observed in neat PVDF, 70/30 blend and 30/70 blend when crystallized at 155°C, without γ crystals. The band period of PVDF α spherulites increases with crystallization temperature as well as the amount of PBS content. At 140°C, spherulites in neat PVDF lose their ring banded feature, while coarse spherulites consisting of evident lamellar bundles could be found in 30/70 blend.

Keywords: Poly(butylene succinate); Poly(vinylidene fluoride); Miscible blends; Morphology and structure.

INTRODUCTION

A common way to control or tailor the properties of materials is to mix two or more components together, resulting in a blend whose behavior is quite different from each of them in many aspects. In the system of small molecules, the mixing could be within individual crystals or within glass since the small size of the molecules allows the energy of geometrical or chemical mismatch between molecules to be confined in a small volume. For polymers, the mixing within a crystal is impossible, since the effect of local mismatch through the crystal could create large increase in the internal energy owing to the strong covalent bonding extending over enormous distances along polymer chains. Therefore, solid polymer blends would be as intimately mixed crystals of the components[1].

Among the large amount of polymeric mixtures, those involving semicrystalline polymers are of particular interest. This is not only because a certain degree of crystallinity is important in order to ensure satisfactory high-temperature strength and environmental resistance, but also because semicrystalline polymer blends offer another system for studing crystallization and morphology of polymers. In the last two decades, some of the

* The work was financially supported by the National Natural Science Foundations of China (No. 20974011) and the program of Introducing Talents of Discipline to Universities (No. B08003).
** Corresponding author: Hui-hui Li (李慧慧), E-mail: lihuihui@mail.buct.edu.cn
Received April 25, 2011; Revised July 1, 2011; Accepted July 6, 2011
doi: 10.1007/s10118-012-1122-6

investigated systems represented the mixture in which one of the components is crystallizable[2–13]. Crystallization in such polymer blends can proceed along a large number of solidification paths which result in a huge variety morphologies and supermolecular structures. These features are interesting from the underlying thermodynamics and rheology which govern the crystallization kinetics, as well as their impact on the materials properties. What happens in a particular case will depend on the miscibility of the components, *i.e.*, whether they are miscible in the whole accessible composition and temperature range or form separated phases. For the immiscible blends, fractionated crystallization usually happens. The components exist in such blends as pure polymers side by side as individual phase, building a particular phase separated structure. For the blends with miscibility gap, interface crossing crystallization could be observed. In such blend systems, the two phases have different contents of crystallizing component, the phase with higher content of the crystallizing component starts to crystallize before the second one. Upon reaching the interface, secondary nucleation induced crystallization in the second phase occurs. This interface crossing crystallization may consequently lead to a number of interesting and strange structures, which will cause a good adhesion between the two phases and may be therefore important for the mechanical property.

PVDF is a representative material with a variety of crystal modifications and attracts much attention due to its outstanding electroactive properties. PBS is a biodegradable polymer with environmental and ecological advantages. Both of them are crystalline polymers, with a melting point gap of about 60 K, and with good miscibility. Ikehara *et al*.[14] have first reported the miscibility of the PVDF/PBS blend. Also, the crystallization behavior of the blend was studied by DSC and optical microscopy. Later on, the structural changes on a lamellar scale of this miscible crystalline polymer blend system during melting and crystallization processes have been investigated by Kaito *et al*.[15, 16] *via* real-time small angle X-ray scattering measurements. In the present work, PVDF/PBS has been chosen again as a model system, and the morphological development of PVDF in the blend under various conditions was visualized by optical microscopy on a micrometer scale and atomic force microscopy on a lamellar resolved scale. The effect of PBS on the morphology evolution of PVDF in the blends has been discussed.

EXPERIMENTAL

Materials and Sample Preparation

PVDF and PBS used in this work were purchased from Sigma-Aldrich Company and have a weight-average molecular weight of about 2.7×10^5 and 6.3×10^4, determined by gel permeation chromatography (GPC) with eluants of *N*,*N*-dimethyl formamide (DMF) and chloroform, respectively. The melting points were measured to be 186°C for PVDF and 120°C for PBS. Both of them were used as received. Blends of PVDF and PBS were prepared by solution blending. Both of them were dissolved in DMF, which serves as a common solvent, with desired mass proportions (total polymer concentration was 20 mg/mL). Thin films for optical microscopy (OM) and atomic force microscopy (AFM) observations were prepared by solution casting and spin-coating on glass slides, respectively. These films were allowed to dry under vacuum at 50°C for 3 days. The thicknesses of the resultant films were estimated to be 10 μm for OM and 600 nm for AFM observations. The obtained films were heat-treated to 200°C for 3 min to erase the thermal history of the samples and subsequently cooled to predetermined isothermal crystallization temperatures. To reveal the influence of PBS on PVDF, the crystallization of PVDF was conducted at temperatures above the melting point of PBS.

Characterization

An Olympus BH-2 microscope equipped with a Linkam LK-600PM temperature controller was used in this study to observe the crystallization process and spherulitic morphology. All of the optical micrographs shown in this paper were taken under crossed polarizers. Tapping-mode AFM images were obtained in the repulsive force region using a NanoScope III MultiMode AFM (Digital Instruments) equipped with a high-temperature heating accessory (Digital Instruments). Si cantilever tips (TESP) with a resonance frequency of approximately 300 kHz and a spring constant of about 40 N m^{-1} were used. The scan rate varied from 0.7 Hz to 1.2 Hz with a scan

density of 512 lines/frame. The set-point amplitude ratio, A_{sp}/A_0, was adjusted to 0.6–0.9, where A_{sp} is the set-point amplitude and A_0 is the amplitude of the free oscillation. All the optical micrographs and AFM images are taken at 125°C (higher than the T_m of PBS).

RESULTS AND DISCUSSION

Since the degree of supercooling and the content of PBS serve as key factors influencing the crystal structures and morphologies of PVDF in the blends, so in this part we will follow these two clues to study the morphological development of PVDF component under different crystallization temperatures in both PVDF-rich and PBS-rich blends. To better understand the morphological changes of PVDF in the blends, pure PVDF crystallized at 170°C is first presented in Fig. 1(a). One sees that PVDF forms typical large γ form spherulites of hundreds of microns in diameter with extraordinarily weak birefringence[17, 18]. In some cases, ring banded structures corresponding to the α form crystals could be observed at the center part of the γ-PVDF spherulites (indicated by an arrow in Fig. 1a). It should be pointed out that the γ form of PVDF, which creates at low degree of supercooling, is a thermodynamically stable phase, while the α form is preferential in kinetics. When PVDF crystallizes at high temperatures, ring banded α form spherulites could start to grow first and subsequently more stable γ form crystals begin to take place in succession. Adding 30% of PBS makes the morphologies of PVDF spherulites change significantly. As shown in Fig. 1(b), the PVDF in a 70/30 PVDF/PBS blend exhibits intrigued flower-like spherulitic morphology. *In situ* growth experiment shows that the PVDF crystallization undergoes three growth steps as referred by the numbers in Fig. 1(b), which starts from the center of the spherulite resulting in the ring banded structures, the bright short leaves in the middle and the long dark leaves outside, respectively. With careful inspection, one could find the crevice between PVDF spherulites. Further decreasing the temperature to enable the crystallization of PBS confirms that the crevice is filled with PBS melt (Figure not shown here). This is reasonable since high diffusion ability of PBS chains at high temperatures leads to the slowly growing PVDF spherulites to expel the PBS melt gradually into their growth front and finally enrich the crevice. Figure 1(c) shows the 30/70 blend crystallized isothermally at 167°C for 100 h. Seldom spherulites could be seen due to the lower nucleation ability of PVDF in PBS-rich blend. In this case, only large α spherulites are observed, no γ spherulites could be found, indicating the existence of large amount of PBS favors the formation of α spherulites. This phenomenon could be expected since the adding of PBS changes the stress on PVDF lamellar surface and results in the twisting of the lamellae. It should be mentioned that the α-PVDF structures in Figs. 1(a), 1(b) and 1(c) have transformed simultaneously during crystallization process into its γ' form through a solid-solid phase transition under high temperatures[18, 19], which has been verified by the increase of their melting points (Refers Fig. 3b).

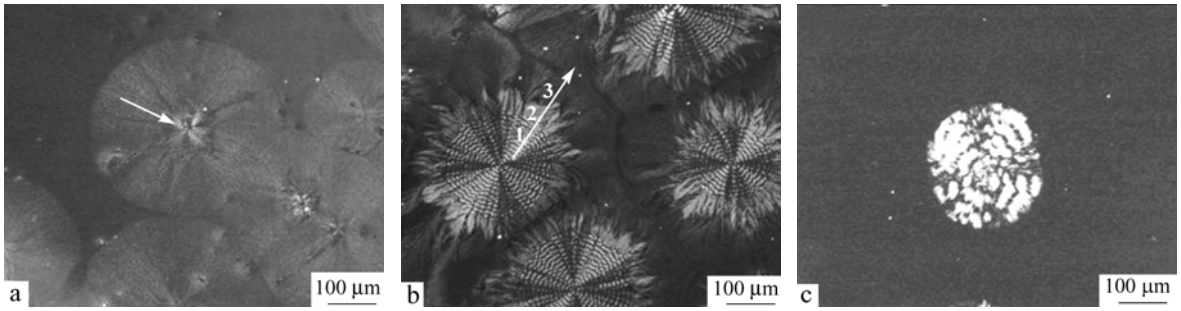

Fig. 1 Optical micrographs showing the morphologies of (a) neat PVDF crystallized isothermally at 170°C, (b) the PVDF in a 70/30 PVDF/PBS blend crystallized isothermally at 167°C and (c) the PVDF in a 30/70 PVDF/PBS blend crystallized isothermally at 167°C for 100 h
The white arrow in (a) indicates the banded structures of PVDF, while the arrow and numbers in (b) indicate the growth direction and the different morphologies corresponding to the three growth steps; The PBS in parts (b) and (c) were in melt.

To better understand the different morphologies of PVDF shown in Figs. 1(a) and 1(b), we studied their fine structures by using AFM on a lamellar resolved scale, as shown in Fig. 2. Figure 2(a) shows closely packed lamelli-form crystals seen face-on, which are the predominate structures in γ form of PVDF spherulites grown at 170°C. Such extraordinary crystallographic regularity together with the packing manner of the chains in its unit cell make the *c* axes (chain axes) of the PVDF crystals inclined at a small angle with respect to the incident light, which leads to consequently a sharp decrease in birefringence. In the case of Fig. 1(b), one sees the core of each PVDF spherulite is typical ring banded crystals followed by two kinds of "leaves" with different birefringence intensity growing outward. The AFM observations have helped to show their lamellar organization. As shown in Fig. 2(b), in the region designated as "2" in Fig. 1(b), random oriented densely packed lamellae with both edge-on and flat-on orientation are observed, which results in an increment of the birefringence. On the other hand, the region numbered as "3" in Fig. 1(b), see Fig. 2(c), shows lamellar structure similar to what we see in Fig. 2(a) but with loosely packed flat-on lamellae (compare Fig. 2a and Fig. 2c), indicating again the dissipation of materials. Taking the above morphological features into account, the growth mechanism of PVDF crystals in Fig. 1(b) can be explained as follows: as the ring banded α crystals growing, the PVDF chains in the growth front arrange into the crystal lattice, which rejects the molten PBS into the growth front. So the concentration of PVDF in the growth front decreases, resulting in the increase of supercooling and formation of thermodynamically stable γ phase (the bright short leaves). At the last stage of growing, dissipation of PVDF makes the crystals growing in the most material-saving way that generates the crystals seen in Fig. 2(c).

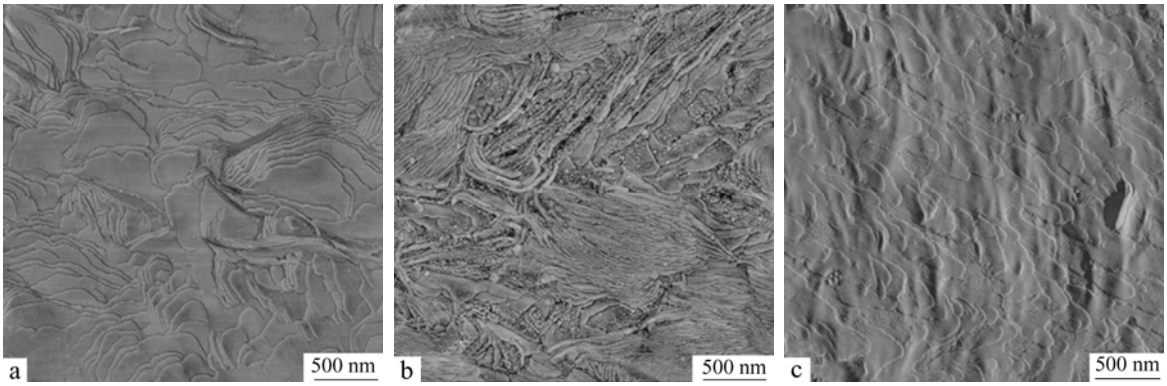

Fig. 2 (a) AFM phase image of the crystal surface of the non-banded γ-PVDF in Fig. 1(a),
(b) and (c) the AFM phase images obtained in the areas numbered as "2" and "3" of Fig. 1(b), respectively

Figure 3(a) shows neat PVDF crystallized at 165°C. Ring banded α form spherulites and γ form spherulites with weaker birefringence coexist at this time. Such morphological features are very common in the intermediate crystallization temperature range. In order to know whether the $\alpha \rightarrow \gamma'$ phase transition occurs, we carry out *in situ* temperature varying experiment since the melting point of γ' phase is higher than both α and γ phases. As shown in Fig. 3(b), after heating to 186°C, almost all of the formed α-PVDF crystals, except for a strip of crystals adjacent to the γ phase, have been melted. The remaining strip indicates the occurrence of $\alpha \rightarrow \gamma'$ phase transition. When the temperature further increased to 195°C, the γ phase melts with the strip of γ' crystals left. This result has proved the model proposed by Lovinger[18] that existing of γ crystals could induce $\alpha \rightarrow \gamma'$ phase transition from the boundary backward to the center of the α spherulite.

Figure 4(a) shows the spherulitic morphologies of PVDF in a 70/30 PVDF/PBS blend crystallized completely at 162°C. The banded α form spherulites, in their turn, get coarser compared with compact ones for the neat PVDF (Fig. 3a), and become much open and irregular as looking away from the center to the outer (see the dotted arrow in Fig. 4a). This results from the dilute effect after blending with PBS. At the place farther and farther away from the center of the spherulites, more and more PBS was accumulated due to the exclusion by

growing PVDF spherulites. This leads to the formation of coarser fibrils along the radial direction of the spherulites. What's more, the occurrence of none volume-filling spherulites of PVDF caused by materials impoverishment also indicates the strong exclusion and enrichment of PBS component in the rest melt. As for the γ spherulites, a uniform increment of the birefringence happens in the blend with respect to the ones in neat PVDF, as seen in Fig. 4(a). This is again related to the inner structure changes of the γ form crystals in the blend, which has been confirmed by AFM (Figure not shown since it looked very similar to that of Fig. 2b). It is worth to note that the $\alpha \rightarrow \gamma'$ phase transition in the blend is somewhat different from that of the neat PVDF. As the solid arrow shown in Fig. 4(a), these banded structures located in the center of α spherulites are confirmed to be γ' phase by temperature varying experiment, which implies that the $\alpha \rightarrow \gamma'$ phase transition starts from the centers of the spherulites in the blend other than in the boundary between α and γ phases that is typical for the neat PVDF. When the PBS content increased up to 70%, *i.e.* in the 30/70 PVDF/PBS blend, both α and γ form spherulites become much coarser and more open than ever before, as shown in Fig. 4(b). The bunch of the fibrils in γ spherulites could also be seen. The existence of the crystal free space, which hardly changes or at most changes quite slowly with extending time, implies the existence of large amount of PBS in the melt.

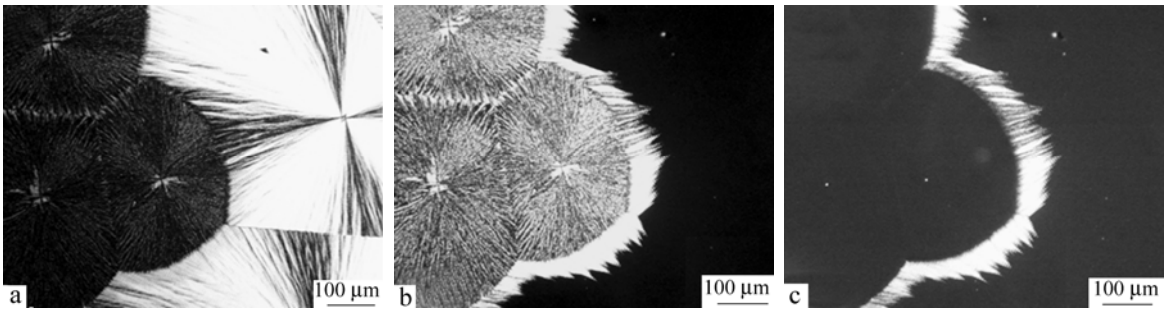

Fig. 3 Optical micrographs of neat PVDF (a) crystallized at 165°C and then (b) melt at 186°C (melting of α-PVDF) and (c) 195°C (melting of γ-PVDF)

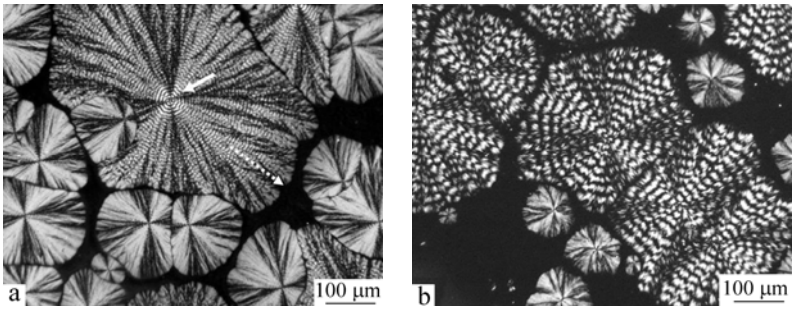

Fig. 4 Optical micrographs of PVDF in (a) 70/30 PVDF/PBS blend crystallized completely at 162°C and (b) 30/70 PVDF/PBS blend crystallized at 162°C for 100 h
The dotted arrow in (a) indicates that the spherulite gets more open with increasing distance from the spherulite center, while the solid arrows indicate the γ' crystals transformed from the ring banded α phase.

Figures 5(a)–5(c) show the morphologies of PVDF in the 100/0, 70/30 and 30/70 PVDF/PBS blends crystallized at 155°C, respectively. Spherulites with evident ring banded structures could be seen in all the cases, no γ phase PVDF crystals have been observed. In this case, the crystallization temperature is also too low to induce the $\alpha \rightarrow \gamma'$ phase transition. We also find that the size of the spherulites increases with increasing of PBS content, implying relative low nucleation ability of PVDF after blending with PBS. Moreover, for the blends, the spherulitic structures become looser with coarse fibril bundles. What's more, the typical Maltese-crosses become weak in the blend and the boundaries between spherulites become not smooth and even nonlinear when

the PBS reaches 70%. However, the remaining space between PVDF spherulites in both blends is limited as can be seen in Figs. 5(b) and 5(c). This indicates that most of the molten PBS was expelled into the interlamellar and interfibrillar regions of the PVDF spherulites instead of the interspherulitic regions as in the case of Fig. 4.

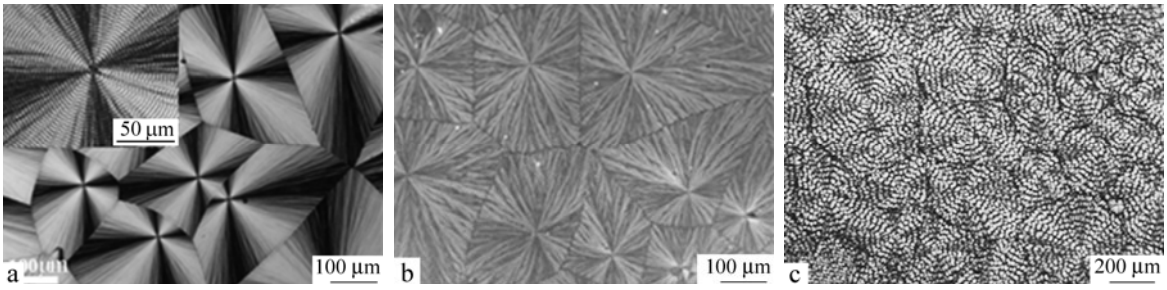

Fig. 5 Optical micrographs of PVDF in (a) 100/0, (b) 70/30 and (c) 30/70 PVDF/PBS blends crystallized at 155°C The insert in (a) is an enlarged part of the banded spherulite.

According to the morphological observation, several aspects should be addressed. We first concern the influence of blending PBS on the band periodicity of PVDF spherulites in the α form. Figure 6 shows the changes of the band periodicity of α-PVDF spherulites as a function of blend ratio and crystallization temperature. It is evident that the band periodicity increases with crystallization temperature as well as the amount of PBS content. The increase of band periodicity with temperature is expected as frequently reported for many other polymer systems with extinction feature[20–23]. However, the increase of band periodicity with the increase of the second component is quite different from the results of other blend systems, where a reduction in band spacing is usually obtained[24, 25], although with a few of exceptions[26, 27]. It is generally accepted that the band periodicity depends on the chain mobility, crystal growth rate and surface free energy[22]. In this case, PBS act as solvent for PVDF due to the good compatibility between these two components. This results in an increment in chain mobility of PVDF, which may contribute to the increment of band periodicity in PVDF spherulites.

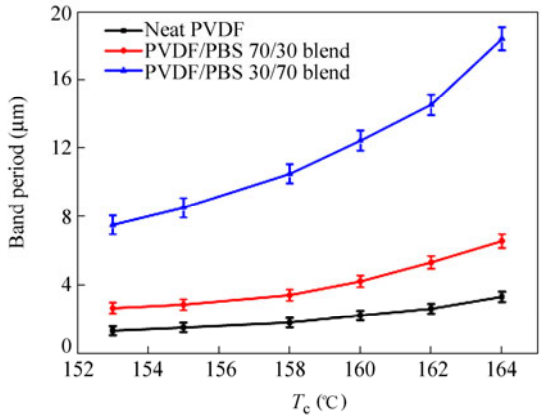

Fig. 6 Variation of band periodicity of PVDF banded spherulites in PVDF/PBS blends with different blend ratios as a function of crystallization temperature

Second, we concern the inner structure of the ring banded PVDF spherulites formed in neat PVDF and the blend samples. For the neat PVDF, the AFM phase image, see Fig. 7(a), shows alternate arrays of edge-on and flat-on lamellae coexist along the radial direction with their boundary clearly delineated, which means no gentle continuous twist of the lamellar orientation. This twisting habit with sudden change in *c*-axis orientation of the lamellae is somewhat different from that of other polymers with ringed structure, *e.g.* PEA[26], which is usually

caused by changing of lamellar orientation gradually along radial direction. This result confirms the previous study on the ring patterns of PVDF by electron microscopy[28]. Nevertheless, this kind of lamellar twisting is fairly regular along the radial direction on the whole, and therefore responsible for the formation of well ordered banded structures shown in Fig. 5(a). Figure 7(b) shows the representative AFM phase image of PVDF spherulites in 70/30 blend. Scanning was taken at 125°C (above the melting temperature of PBS). Alternate arrays of edge-on and flat-on lamellae have also been seen coexisting in the scan area, which is typical lamellar organization model for banded spherulites. Compared with banded structures in neat PVDF (Fig. 7a), the boundary between edge-on and flat-on lamellae is now not sharply delineated. With careful inspection, continuous twist of some single lamellar sheets from flat-on into edge-on orientation and vice versa is discernable as indicated by the arrows in Fig. 7(b). There exist numerous crevices in the interlamellar regions as well as non-crystallized pockets located in the interfibrillar area where the PBS melt is held.

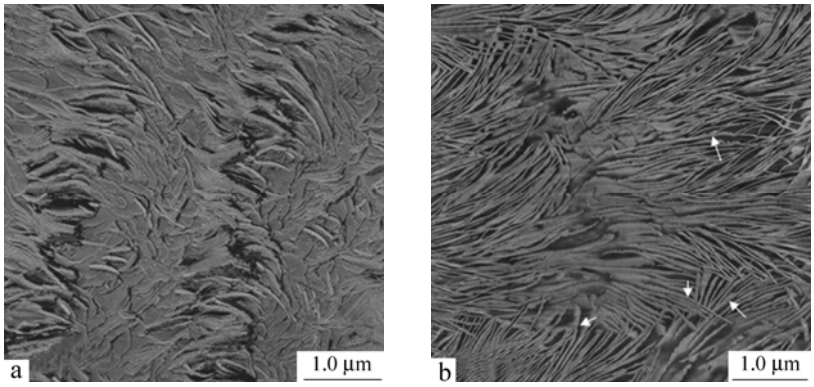

Fig. 7 AFM phase images of the samples used in (a) Fig. 5(a) and (b) Fig. 5(b)
The arrows in (b) indicate the twisted single lamellar sheets; Scanning is taken at 125°C.

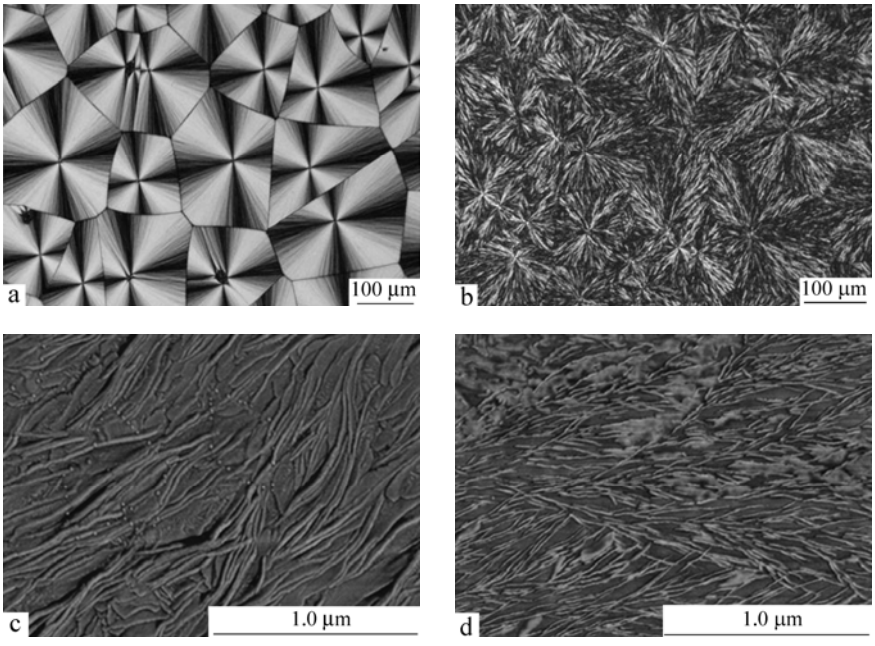

Fig. 8 (a) Optical micrographs of neat PVDF and (b) 30/70 PVDF/PBS blend crystallized at 140°C, (c) and (d) the AFM phase images of (a) and (b), respectively
Scanning is taken at 125°C.

When the PVDF was crystallized at 140°C, Fig. 8(a), compact spherulites with clear Maltese-crosses were obtained. They have linear boundaries and completely lose their ring banded feature under such a high supercooling. On the other hand, when the PVDF in the 30/70 PVDF/PBS blend was crystallized at the same temperature, *i.e.* 140°C, coarser spherulites developed (Fig. 8b). These coarse spherulites consisting of lamellar bundles with a large cross section and the Maltese-crosses are completely lost, suggesting a random arrangement of lamellar bundles caused by the exclusion of PBS from the lamellar bundles of PVDF. This kind exclusion of noncrystalline component from the lamellar bundles has been confirmed by the small-angle X-ray scattering experiments in the system of PMMA/PVDF[29]. In this case, we also use AFM to measure the lamellar structure of both the neat PVDF and PVDF in 30/70 blend, as shown in Figs. 8(c) and 8(d). An admixture of edge-on and flat-on lamellae could be seen coexisting in Fig. 8(c). They are densely packed with random orientation. This is the reason for losing the ring banded feature (see Fig. 8a). As for Fig. 8(d), one can find that the lamellar organization becomes loosened and the branched lamellae bundles, *i.e.* the fibrils with many intrafibrillar/interfibrillar molten pockets between them. These pockets are the exact places where the PBS melt is.

CONCLUSIONS

In summary, we systematically investigated the effect of PBS on the morphological features of PVDF by optical and atomic force microscropies under various conditions. It was found that neat PVDF forms large γ form spherulites with extraordinarily weak birefringence at 170°C. These spherulites are composed of closely packed face-on lamellae. Adding 30% PBS leads to the formation of intrigued flower-like spherulitic morphology of PVDF, which is composed of ring banded structures in the core, the bright short leaves in the middle and the long dark leaves outside. AFM measurement shows the bright short leaves consist of aggregate of lamellae with random orientation, while loosely packed flat-on lamellae are the dominated structure in long dark leaves. We suggest that this growth mechanism results from the decrease of supercooling and materials dissipation. Increasing the PBS content to 70% favors the formation of ring banded spherulites and decreases the nucleation ability of PVDF. Well organized ring banded α spherulites with some γ crystals could be seen when crystallize the PVDF at 165°C, *in situ* temperature varying experiment verifys the occurrence of $\alpha \rightarrow \gamma'$ phase transition from the junction sites of α and γ crystals backward to the center of the α spherulite. Blending of 30% PBS results in the PVDF α spherulites getting coarser and much open as the distance from the center increases. The PBS, in this case, is strongly excluded and enriched in the interspherulitic region. The $\alpha \rightarrow \gamma'$ phase transition at this time starts from the centers of the α spherulites. Both the α and γ form spherulites become even more open and irregular than ever before when PBS content increases up to 70%, the formation of the crystal free space implies the existence of large amount of PBS in the melt. Dominated ring banded structures could be observed in neat PVDF, 70/30 blend and 30/70 blend crystallized at 155°C, no γ crystals could been seen. The crystallization temperature in this case, is too low to initiate the $\alpha \rightarrow \gamma'$ phase transition. Most of PBS is expelled into the interlamellar and interfibrillar regions of the PVDF spherulites. Systematic measurement shows the band period of PVDF α spherulites increases with crystallization temperature as well as the amount of PBS content. AFM test shows alternate arrays of edge-on and flat-on lamellae coexist in neat PVDF with their boundary clearly delineated, while the boundaries are not sharply delineated in 70/30 blend. Continuous twisting of some single lamellar sheets from flat-on into edge-on orientation has been observed. At 140°C, spherulites in neat PVDF completely lose their ring banded feature while coarse spherulites consisting of evident lamellar bundles could be found in 30/70 blend. AFM measurement shows an admixture of edge-on and flat-on lamellae existing in neat PVDF. For 30/70 blend, the lamellar organization becomes loosened and the branched lamellae bundles with many intrafibrillar/interfibrillar molten pockets between them could be seen. These pockets are the exact places where the PBS melt is.

REFERENCES

1 Schultz, J.M., Front. Chem. China, 2010, 5: 262
2 Morra, B.S. and Stein, R.S., Polym. Eng. Sci., 1984, 24: 311
3 Russell, T.P. and Stein, R.S., J. Polym. Sci., Polym. Phys. Ed., 1983, 21: 999
4 Briber, R.M. and Khoury, F., Polymer, 1987, 28: 38
5 Hahn, B., Hermann-Schonherr, O. and Wendorff, J., Polymer, 1987, 28: 201
6 Silverstre, C., Karasz, F.E., MacKnight, W.J. and Martuscelli, E., Eur. Polym. J., 1987, 23: 745
7 Russell, T.P., Ito, H. and Wignall, G.D., Macromolecules, 1988, 21: 1703
8 Su, Y., Wang, K., Zhang, Q., Chen, F. and Fu, Q., Chinese J. Polym. Sci., 2010, 28(2): 249
9 Wei, J., Sun, J., Wang, H., Chen, X. and Jing, X.B., Chinese J. Polym. Sci., 2010, 28(3): 499
10 Hu, H.X., Sgangguan, Y.G., Zuo, M. and Zheng, Q., Acta Polymerica Sinica (in Chinese), 2009, (2): 123
11 Luo, F.L., Zhang, X.Q., Li, R.B., Fu, D.S., Gan, Z.H., Ji, J.H. and Wang, D.J., Acta Polymerica Sinica (in Chinese), 2009, (10): 1043
12 Wu, N.J. and Yang, P., Acta Polymerica Sinica (in Chinese), 2010, (3): 316
13 Yang, J., Wang, Z.B., Wu, Y., Wu, X.F. and Gu, Q., Acta Polymerica Sinica (in Chinese), 2010, (8): 987
14 Ikehara, T., Kimura, H. and Qiu, Z., Macromolecules, 2005, 38: 5104
15 Li, Y., Kaito, A. and Horiuchi, S., Macromolecules, 2004, 37: 2119
16 Kaito, A., Shimomura, M., Akaba, M. and Nojima, S., J. Polym. Sci. Part B: Polym. Phys., 2007, 45: 1959
17 Gregorio, R. and Cestari, M.J., Polym. Sci., Part B: Polym. Phys., 1994, 32: 859
18 Lovinger, A., Polymer, 1980, 21: 1317
19 Braun, D., Jacobs, M. and Hellmann, G.P., Polymer, 1994, 35: 706
20 Wang, Z.G. and Jiang, B.Z., Macromolecules, 1997, 30: 6223
21 Su, C. and Lin, J.H., Colloid. Polym. Sci., 2004, 283: 188
22 Xu, J., Guo, B., Chen, E., Zhou, J., Li, L. and Wu, J., Polymer, 2005, 46: 9176
23 Wang, H.J., Gan, Z.H., Schultz, J.M. and Yan, S.K., Polymer, 2008, 49: 2342
24 Wang, Z.G., Wang, X.H., Yu, D.H. and Jiang, B.Z., Polymer, 1997, 38: 5899
25 Xiao, Q., Yan, S., Rogausch, K.D., Petermann, J. and Huang, Y., J. Appl. Polym. Sci., 2001, 80: 1684
26 Wang, T. and Yan, S., Phys. Chem. Chem. Phys., 2009, 11: 1622
27 Penning, J.P., St. J. Manley, R., Macromolecules, 1996, 29: 77
28 Bassett, D.C., Proc. R. Soc. Lond. A, 1961, 377: 61
29 Saito, H. and Stuhn, B., Macromolecules, 1994, 27: 216